JACS
JOURNAL OF THE AMERICAN CHEMICAL SOCIETY
pubs.acs.org/JACS
Article

Discrete Libraries of Amphiphilic Poly(ethylene glycol) Graft Copolymers: Synthesis, Assembly, and Bioactivity

Junfeng Chen, Aoon Rizvi, Joseph P. Patterson, and Craig J. Hawker*

Cite This: https://doi.org/10.1021/jacs.2c07859
Read Online

ACCESS | Metrics & More | Article Recommendations | Supporting Information

ABSTRACT: Poly(ethylene glycol) (PEG) is an important and widely used polymer in biological and pharmaceutical applications for minimizing nonspecific binding while improving blood circulation for therapeutic/imaging agents. However, commercial PEG samples are polydisperse, which hampers detailed studies on chain length-dependent properties and potentially increases antibody responses in pharmaceutical applications. Here, we report a practical and scalable method to prepare libraries of discrete PEG analogues with a branched, nonlinear structure. These lipid-PEG derivatives have a monodisperse backbone with side chains containing a discrete number of ethylene glycol units (3 or 4) and unique functionalizable chain ends. Significantly, the branched, nonlinear structure is shown to allow for efficient nanoparticle assembly while reducing anti-PEG antibody recognition when compared to commercial polydisperse linear systems, such as DMG-PEG2000. By enabling the scalable synthesis of a broad library of graft copolymers, fundamental self-assembly properties can be understood and shown to directly correlate with the total number of PEG units, nature of the chain ends, and overall backbone length. These results illustrate the advantages of discrete macromolecules when compared to traditional disperse materials.

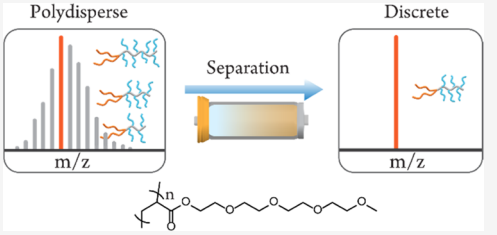

Downloaded via UNIV OF CALIFORNIA SANTA BARBARA on October 18, 2022 at 00:05:04 (UTC).
See https://pubs.acs.org/sharingguidelines for options on how to legitimately share published articles.

INTRODUCTION

The development of discrete and sequence-specific synthetic macromolecules with control over their function and performance is a transformational opportunity in materials science.[1−7] This is particularly true for biological and pharmaceutical applications where single molecular entities are desirable. However, in contrast to discrete biological macromolecules,[8,9] traditional synthetic polymers are characterized by dispersity, with structural variations being observed in backbone molecular weight, chain ends, and branching. Even with the same average molecular weight, synthetic samples may have different molecular structures, which in turn leads to differences in properties and behavior.[10] These advantages for discrete materials versus the ensemble properties observed for disperse systems are especially true for poly(ethylene glycol) (PEG), where broad use in imaging, diagnostics, and drug delivery applications may further enhance the advantages of discrete systems.[11−13]

The importance of synthetic PEG derivatives in bioapplications is exemplified by DMG-PEG2000, where a single lipid group is coupled with a polydisperse, linear PEG chain of average molecular weight, 2000 g/mol. As a PEGylated lipid, DMG-PEG2000 can co-assemble into lipid nanoparticles (LNPs), which exhibit low nonspecific binding, improved cargo stability, and long blood circulation lifetimes. Commercially, DMG-PEG2000 is a key component of the drug delivery system for the Moderna COVID-19 vaccine.[14−16] However, the current commercial system faces two major drawbacks. First, DMG-PEG2000 is polydisperse and subject to batch-to-batch difference (Figure 1a). Polymer chains with different lengths have different metabolic kinetics, biodistribution, and self-assembly properties in the human body, resulting in variable efficacy and concerns on long-term safety. It is also challenging to establish structure−function relationships in biological applications for disperse materials with varying compositions. Second, linear PEG derivatives are widely used in a multitude of other commercial applications ranging from pharmaceutics to personal care. This results in an increased occurrence of anti-PEG antibodies,[17−19] with the percentage of the population with pre-existing anti-PEG antibodies rising from ∼0.2% in 1980 to 72% in 2016.[20−23] A recent study has shown that the levels of anti-PEG antibodies are boosted in humans by SARS-CoV-2 mRNA vaccines containing lipid nanoparticles derived from DMG-PEG2000.[24] Understanding the properties and long-term safety profile for PEG-based bioconjugates through the availability of discrete materials and developing alternate structures by changing the macromolecular architecture are therefore key drivers for future research. In this work, a scalable synthetic strategy is developed to generate libraries of discrete PEG derivatives directly, allowing for fundamental studies to be performed. In the literature, synthetic approaches to discrete PEG derivatives

Received: July 25, 2022

© XXXX American Chemical Society

https://doi.org/10.1021/jacs.2c07859
J. Am. Chem. Soc. XXXX, XXX, XXX−XXX

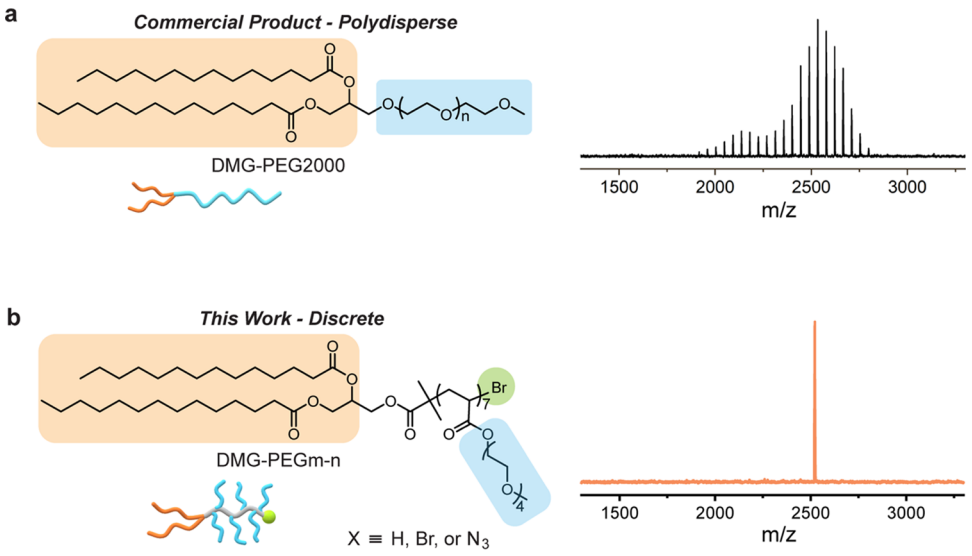

Figure 1. (a) Chemical structure and the MALDI spectrum of DMG-PEG2000 and (b) the chemical structure and MALDI spectrum of discrete PEG oligomers.

have been developed based on stepwise strategies.[25−27] However, these approaches are typically not amenable to the preparation of functional derivatives and are difficult to scale to multigram libraries of higher molecular weight materials. In addition, PEG derivatives are designed with branched architectures that lower anti-PEG antibody binding.

Our group has a long-term interest in developing synthetic strategies for the synthesis of macromolecules with precise control over their structure and dispersity.[28−30] Recently, we have demonstrated chromatographic separation as a platform for both discrete oligomers[31−34] and unique, low-dispersity block copolymer libraries.[35,36] This growing reliance on PEG in a variety of different fields, coupled with increasing sensitization to linear PEG, prompted our group to develop a scalable and versatile strategy for discrete, branched PEG libraries that would allow comparison to well-known systems, such as DMG-PEG2000 (Figure 1). In this approach, functionalized ATRP initiators are used to control the polymerization of tri- or tetra(ethylene glycol)acrylate, with the products being purified by automated chromatography. The utility of this approach is demonstrated through the facile preparation of a library of discrete acrylate-based lipid-PEG conjugates that are structurally analogous to commercial, polydisperse DMG-PEG2000 systems. Although chromatographic separation is novel in polymer science, this technique holds potential in high-value applications, especially for pharmaceutics which require μg to mg quantities per dose.

RESULTS AND DISCUSSION

Design and Synthesis of DMG-PEG Copolymers. The design of discrete PEG graft copolymers with an acrylate backbone was based on the following considerations. PEG derivatives with molecular weights of ∼1000 to 3000 g/mol, which corresponds to ∼20 to 60 ethylene glycol (EG) repeat units, are widely used in biological applications. In addition, chain ends must be controlled, and the presence of branching may lead to decreased biofouling and antibody binding. Traditional strategies for PEG synthesis involve the addition of single EG repeat units leading to incremental changes in the degree of polymerization (DP) and minimal polarity differences. As a result, scalable chromatographic separation is not practical for discrete linear PEG above DP = 10.[37] To address this challenge, an oligomeric monomer approach with tri- or tetra(ethylene glycol)acrylate leading to the sequential incorporation of 3 or 4 EG repeat units coupled with atom transfer radical polymerization (ATRP) was employed (Scheme 1). This not only results in a branched structure,

Scheme 1. Preparation of Branched Lipid-PEG Copolymers through ATRP

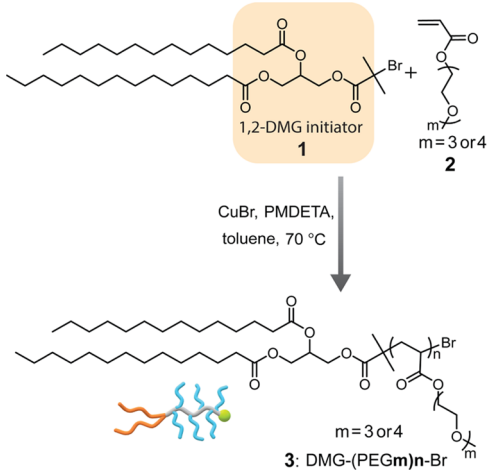

but the number of EG repeat units increases by 3 or 4 units in each series (3, 6, 9, ··· or 4, 8, 12, ··· respectively), which facilitates separation and purification of each library.

The synthesis of discrete PEG copolymers starts with a lipid-based ATRP initiator derived from 1,2-dimyristoyl-glycerol (DMG). It should be noted that DMG derivatives are typically prepared from glycerol and give rise to both the desired 1,2-isomer and the 1,3-DMG isomer due to transesterification. For example, the commercial DMG-PEG2000 material is typically a 97:3 ratio of 1,2-DMG and 1,3-DMG isomers. To exclude the influence of isomeric lipid chain ends in these studies, the 1,3-isomer was removed by repeated recrystallization of the initiator (**1**). While the presence of the 1,3-isomer is difficult to

https://doi.org/10.1021/jacs.2c07859
J. Am. Chem. Soc. XXXX, XXX, XXX−XXX

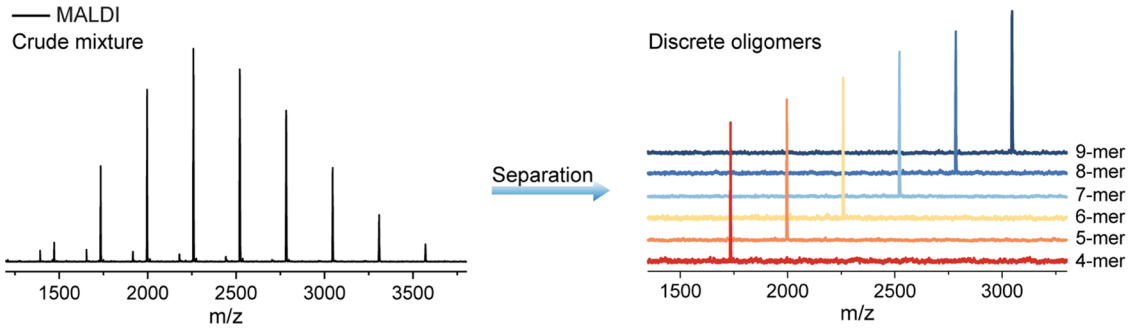

Figure 2. Comparison of MALDI spectra for **DMG-PEG4-Br, 3b**, before and after separation.

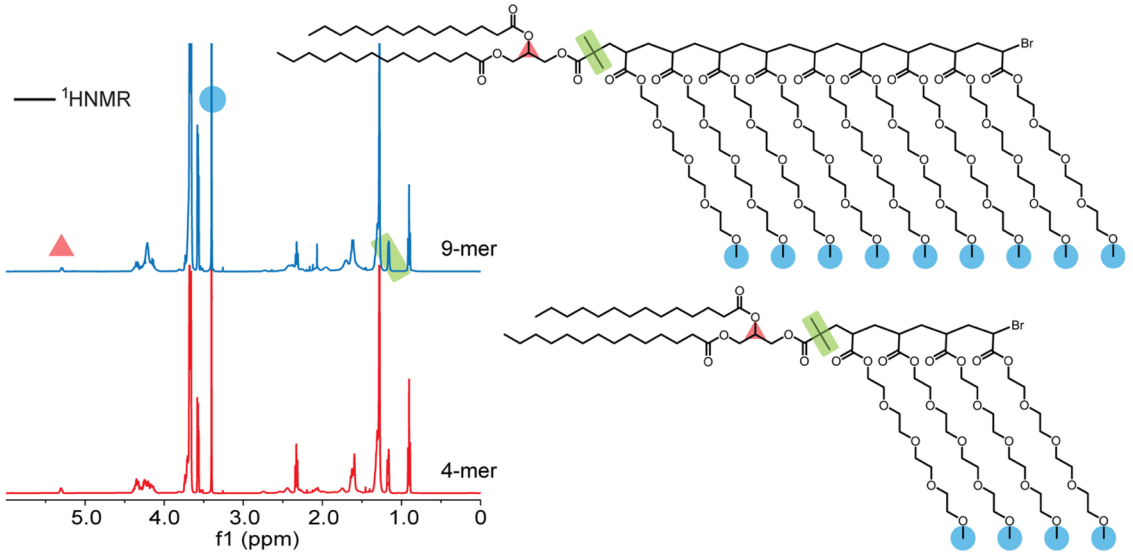

Figure 3. ^{1}H NMR spectra and GPC traces of 4-mer and 9-mer of **DMG-PEG4Br**.

detect by ^{1}H NMR spectroscopy, it was found that high-resolution ^{13}C NMR spectroscopy is a viable method for accurate quantification of isomer purity (Figure S1). Following initiator purification, the copolymer (**3**) was prepared via ATRP using either tri(ethylene glycol)acrylate (**PEG3, 2a**) or tetra(ethylene glycol)acrylate (**PEG4, 2b**) as the monomer and Cu-PMDETA as the catalyst. The crude copolymer products were characterized by ^{1}H, ^{13}C NMR, and gel permeation chromatography (GPC) and, in all cases, shown to have an average DP of n = 6−7 ($Đ$ = 1.07−1.08).

Separation and Characterization of the Discrete Copolymers. Key to the success of this automated chromatography approach is the use of mixed solvent systems, which allows for the optimization of copolymer separation based on the total number of EG units. This allows for discrete copolymer libraries to be obtained in gram quantities for each series studied. For example, **DMG-PEG3-Br**, **3a**, was fractionated to give six discrete species, each having a single DMG and bromo chain end with the oligomer length ranging from 4-mer to 9-mer (12−27 EG repeat units in total). As a result, from 3.0 g of crude **DMG-PEG3-Br**, **3a**, 120−290 mg of each discrete oligomer was obtained. The versatility of this approach was similarly demonstrated through the scalable synthesis and separation of the corresponding series based on tetra(ethylene glycol), **DMG-PEG4-Br**, **3b**, which gives discrete analogues of DMG-2000 with 12−36 EG units.

The structural purity of each copolymer library was determined using GPC, NMR, and matrix-assisted laser desorption/ionization (MALDI) mass spectrometry. For example, representative data for **DMG-PEG4-Br, 3b**, is shown in Figure 2, where the initial mixture shows a series of molecular ions from 3-mer to 11-mer. Chromatographic separation on a multigram scale allows discrete copolymers to be obtained with the purified materials showing molecular ion peaks corresponding to the discrete copolymers with defined chain ends. The power of this approach is exemplified by **DMG-(PEG4)$_9$-Br**, where a set of molecular ion peaks is observed for the 9-mer at 3043 amu, which corresponds to nine tetra(ethylene glycol)acrylate repeat units (36 EG units) as well as single DMG and bromo chain end groups.

Further characterization using a combination of ^{1}H NMR and FT-IR spectroscopy proved to be diagnostic within each library, with specific peaks showing systematic changes as the oligomer length increased. This is illustrated in Figure 3, where ^{1}H NMR spectroscopy shows unique resonances for the single methyne CH of the DMG chain end at ∼5.3 ppm and the multiple methoxy groups for the grafted PEG chains at ∼3.4 ppm. As a representative example, quantitative integration of these peaks for the 4-mer, **DMG-(PEG4)$_4$-Br**, and 9-mer, **DMG-(PEG4)$_9$-Br**, gives ratios of 1:12 and 1:26. This closely matches the expected integration values of 1:12 and 1:27 for the discrete molecular structures.

The presence of a synthetically accessible, single bromo chain end further illustrates the utility of this ATRP strategy for preparing libraries of discrete PEG analogues. As shown by MALDI mass spectroscopy analysis (Figure 4), the bromo

https://doi.org/10.1021/jacs.2c07859
J. Am. Chem. Soc. XXXX, XXX, XXX−XXX

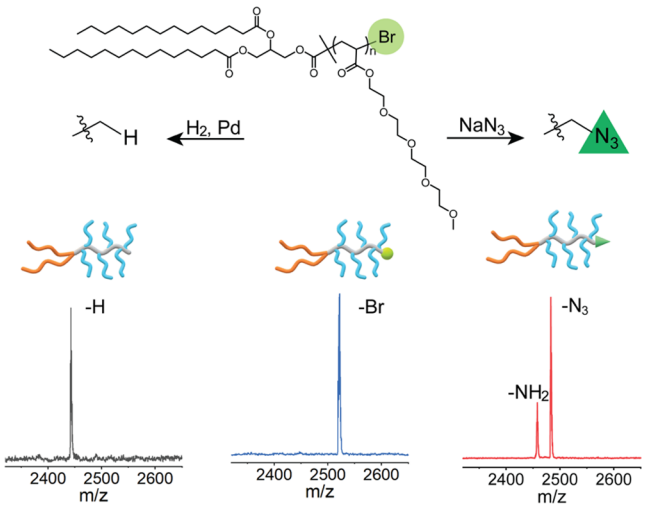

Figure 4. Chain end modifications of the lipid-PEG conjugates. The $-NH_2$ peak was the result of N_3 degradation induced by the MALDI laser.

chain end can be quantitatively removed to give a H-chain end, **DMG-(PEG4)$_7$-H**, through Pd-catalyzed hydrogenation or converted to the corresponding azido group, **DMG-(PEG4)$_7$-N$_3$**, by NaN_3 substitution. As detailed below, the introduction of an azido group opens up a variety of functionalization pathways using click coupling.

Self-Assembly and LCST Behavior. With lipid nanoparticles (LNPs) playing a key role in the transport and delivery of active compounds, such as DNA/RNA,[38] the availability of discrete lipid-PEG libraries provides a unique opportunity to examine fundamental structure/property relationships. To initially address this question, fluorophore solubilization experiments were performed by mixing aqueous assemblies of the discrete DMG-PEG derivatives with the insoluble fluorophore 1,6-diphenyl-1,3,5-hexatriene (DPH). As expected, with increasing oligomer concentration, the fluorescence intensity was observed to increase, indicating the formation of micellar assemblies with the DMG chain ends forming a hydrophobic core that can solubilize the hydrophobic DPH dye (Figure S9).

Dynamic light scattering (DLS) experiments were then performed for three different DMG-PEG libraries (100 μM in water) from 25 to 65 °C. By examining each discrete derivative within the three libraries, the impact of molecular weight (number of PEG units) and nature of the chain ends on the lower critical solution temperature (LCST) could be determined and a complete understanding of self-assembly obtained.[39,40] A strong correlation between the overall number of EO units and LCST was observed for all oligomer libraries (Figure 5). For **DMG-(PEG3-Br)$_n$, 3a**, the 4-mer (12 EO) and 5-mer (15 EO) derivatives show aggregation at room temperature, while the 6-mer (18 EO) and 7-mer (21 EO) oligomers are micellar assemblies with diameters of 8−10 nm up to 35 °C but undergo an LCST at 45 °C to give nanoassemblies. Further increasing the backbone length to 8-

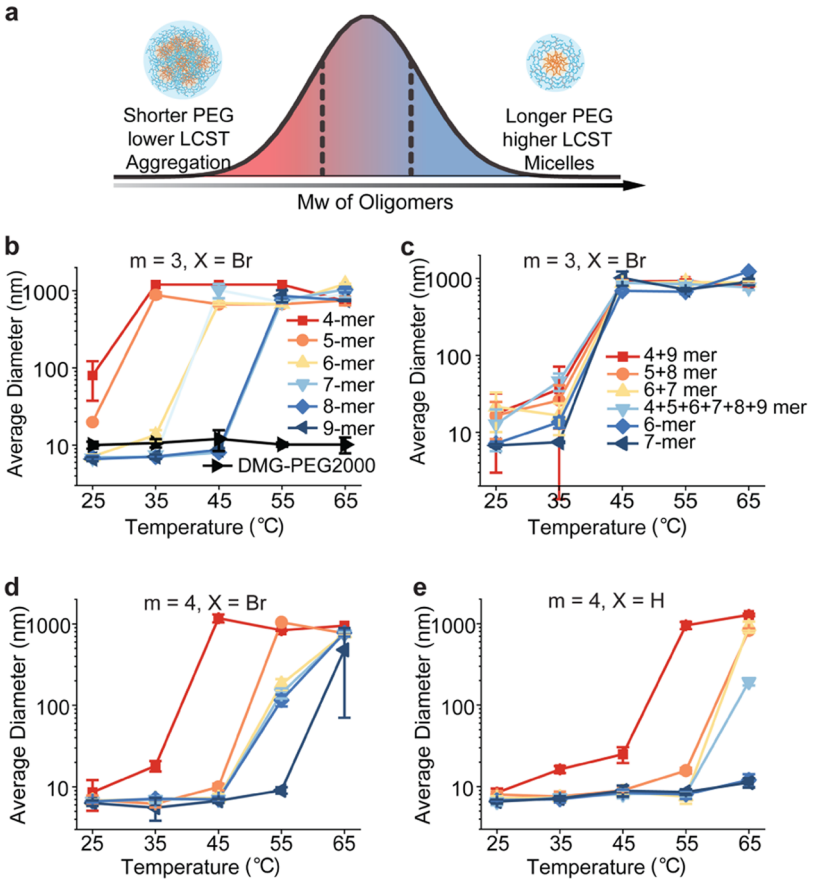

Figure 5. LCST behavior of lipid-PEG micelles in water. (a) Separation of oligomers with different LCST values. (b−e) Micelle diameters measured using DLS in water. [DMG-PEG] = 100 μM.

https://doi.org/10.1021/jacs.2c07859
J. Am. Chem. Soc. XXXX, XXX, XXX−XXX

mer (24 EO) and 9-mer (27 EO) results in an additional rise in LCST to 55 °C. In contrast, the **DMG-(PEG4)$_n$-Br, 3b**, library showed that all oligomers assemble as micelles with diameters of 8−10 nm at room temperature. Only the shortest oligomer (4-mer − 16 EO) shows an LCST at 45 °C with the longer oligomers, 5-mer (20 EO) to 8-mer (32 EO), displaying a broad LCST between 55 °C and 65 °C. For the highest molecular weight 9-mer derivative with the highest number of EO units (36), the LCST is further increased and observed at 65 °C. In comparing the LCST values across and between these different libraries, noticeably different behavior is observed based on the total number of PEG units and their arrangement, either tri(ethylene glycol) or tetra(ethylene glycol) side chains. These detailed insights into structure/property relationships illustrate the power of combining controlled polymerization processes with automated chromatography to give discrete materials.

Further evidence for the utility of this approach can be seen in the dramatically different behavior observed when the single bromo chain is removed to give the corresponding **DMG-(PEG4)$_n$-H, 4a**, library. In direct contrast to the bromo library, multiple oligomeric samples now show no LCST below 65 °C, with only the 4-mer (16 EO) having a broad LCST at 55 °C. These systematic and noticeable changes in assembly properties illustrate the significant influence that small changes in the chain end structure, oligomer length, and overall number of EO units can have on the properties of lipid-PEG systems (Figure 5).

The ability to fine-tune the assembly of these discrete lipid-PEG derivatives may also allow for control over other assembly processes, for example, the synthesis of inorganic nanoparticles.[41−43] To demonstrate this possibility, a systematic study of the oligomer structure on the formation of gold (Au) nanoparticles was conducted.[44,45] In this case, discrete **DMG-PEG4-H** oligomers were used to template nanoparticle formation in the presence of $HAuCl_4$ and $NaBH_4$[46] with UV−vis spectroscopy, DLS, and transmission electron microscopy (TEM), revealing a systematic decrease in UV−Vis absorbance and AuNP diameters with increasing oligomer length (Figure 6). This is highlighted by a comparison of AuNPs prepared in the presence of the 4-mer (16 EO) with AuNPs prepared in the presence of the 9-mer (36 EO). The former was characterized by large nonuniform aggregates with average diameters of ∼20 nm, while the higher molecular weight lipid-PEG derivative led to the formation of uniform NPs with diameters of ∼5 nm. These systematic changes illustrate that the control of the oligomer length and total number of EO units can also be used to accurately regulate the formation and stabilization of inorganic nanoparticles.

Protein/Antibody Binding. A major function of PEGylation is to reduce protein adsorption in bioenvironments, with this stealth effect leading to an increase in the bioavailability of therapeutic and imaging agents. One emerging challenge for PEG-based materials, especially higher molecular weight linear systems, is an increase in anti-PEG antibody responses, which may result in biofouling and a subsequent decrease in efficacy for delivery systems. The availability of these discrete lipid-PEG libraries therefore offers the unique opportunity to understand fundamental relationships between structure and protein adsorption for PEG-based materials.[47]

Protein adsorption with the **DMG-(PEG4)$_n$-H** library was studied using surface plasmon resonance (SPR) measurement.[48,49] As shown in Figure 7, monolayers of the respective

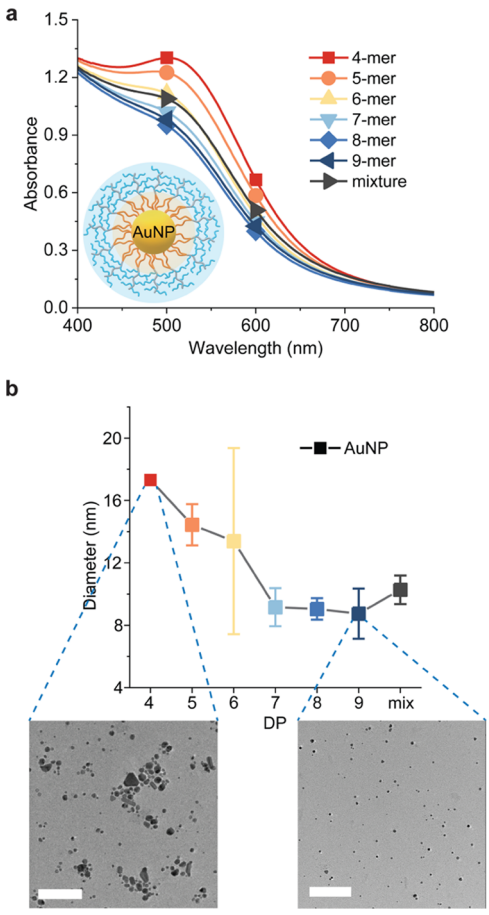

Figure 6. Lipid-PEG-templated gold nanoparticle synthesis. (a) UV−vis spectra of AuNPs prepared under 400 μM of DMG-PEG4H. (b) Hydrodynamic diameters of AuNPs measured using DLS. The inset pictures are captured through TEM; scale bar = 100 nm. The error bar represents the standard derivation of three measurements.

DMG-PEG oligomers were prepared and then exposed to flowing buffer solutions containing either bovine serum albumin (BSA) or anti-PEG antibody. For the protein adsorption studies, the branched PEG showed low BSA binding with 40−60 response unit (RU) compared to ∼1300 RU for the uncoated hydrophobic surface. The binding gradually decreased as the **DMG-(PEG4)$_n$-H** oligomer length increased from the 4-mer (16 EO) to the 7-mer (28 EO), with the level of binding remaining constant as the oligomer length further increased to the 9-mer (36 EO). This behavior is comparable to the BSA binding level for surfaces based on the commercial DMG-PEG2000 system and an artificial mixture of all six discrete oligomers. It is noteworthy that the bromo chain end oligomer, **DMG-(PEG4)$_7$-Br**, showed higher BSA binding when compared to the corresponding **DMG-(PEG4)$_7$-H** derivative, which is consistent with prior results showing the influence of a single chain end. The SPR experiments were also performed with human serum to evaluate the anti-nonspecific binding properties of the PEG samples, and similar results were observed as the BSA tests (Figure S12).

In contrast, the anti-PEG antibody binding showed only a minor but systematic increase in surface binding with increasing oligomer length and overall number of PEG units from 4-mer (16 EO) to 9-mer (36 EO). Significantly, the binding levels for all discrete, branched derivatives were substantially lower (∼5×) than for the commercial, linear

https://doi.org/10.1021/jacs.2c07859
J. Am. Chem. Soc. XXXX, XXX, XXX−XXX

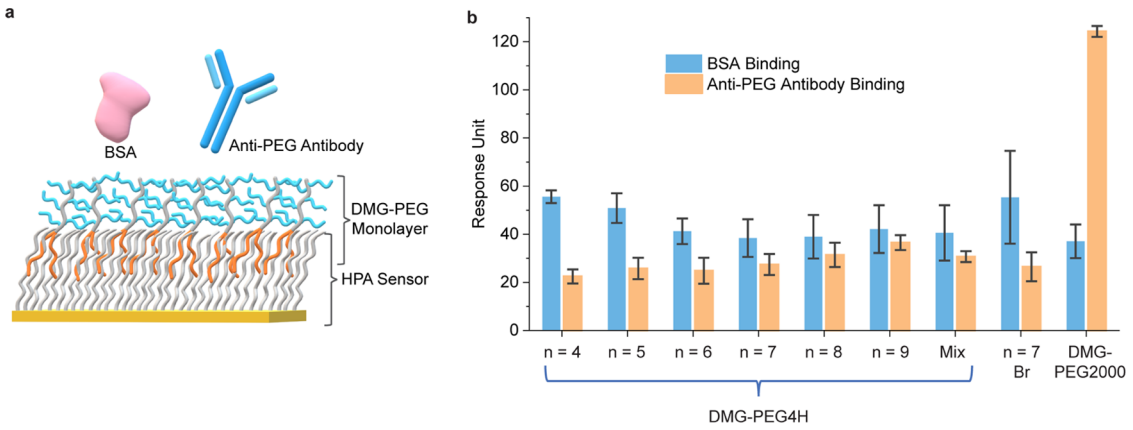

Figure 7. Protein binding studies. (a) Schematic illustration of SPR measurements. (b) BSA and anti-PEG antibody binding measured through SPR experiments. The "mix" contained the mixture of all six discrete oligomers in a 1:1:1:1:1:1 molar ratio. [DMG-PEG] = 500 μM, [BSA] = 0.1 mg/mL, [anti-PEG antibody] = 2 μg/mL. The error bar represents the standard derivation of three measurements.

DMG-PEG2000 system. This dramatic difference supports the hypothesis that the branched PEG copolymer architecture results in lower anti-PEG antibody binding with the graft structure distributing the traditional linear PEG chain into multiple units containing only 4 EGs each, which are believed to be shorter than the epitope recognition of the anti-PEG antibody.[50,51] Combined, these protein adsorption and antibody binding results demonstrate that the discrete, branched lipid-PEG molecules provide a similar level of resistance to protein fouling as traditional linear PEG systems but with a marked decrease in recognition by anti-PEG antibodies.

Lipid-PEG Nanoparticles for DNA/RNA Encapsulation. A major driver for lipid-PEG nanoparticle research is their use as delivery agents for DNA and RNA molecules which are membrane impermeable and unstable in biological environments. As detailed previously, DMG-PEG2000-based nanoparticles have been approved for the encapsulation and delivery of nucleic acids, including COVID-19 mRNA vaccines and siRNA drugs. To illustrate the utility of discrete, lipid-PEG molecules for encapsulation, Calf Thymus DNA[52] was formulated with either **DMG-(PEG4)$_n$-H** or **DMG-(PEG4)$_n$-Br** (n = 4−9) and traditional lipids components 1,2-dioleyloxy-3-dimethylaminopropane (DODMA), 1,2-distearoyl-sn-glycero-3-phosphocholine (DSPC), and cholesterol (Figure 8).

All discrete DMG-PEG oligomers were able to stabilize the encapsulation of 10 wt % DNA with the **DMG-PEG4-H** series showing consistent nanoparticle diameters of ∼100 nm across the full series. Similarly, the **DMG-PEG4-Br** afforded nanoparticles of ∼120 nm for shorter oligomer lengths with diameters approaching that of **DMG-PEG4-H** at longer oligomer lengths (n = 7−9). It is postulated that this indicates the decreasing influence of the hydrophobic bromo chain end for LNP assembly. It is noteworthy that the observed nanoparticle size range of 100−130 nm is within the common range of LNP diameters for commercial systems and has been shown to correlate with efficient delivery.[53] Analysis of the DNA assembles with **DMG-(PEG4)$_7$-H** by cryo-TEM shows the expected LNP structure, which is again similar to traditional systems reported in the literature (Figure 8b). The nucleic acid encapsulation efficiency was then measured using the RiboGreen assay, with 85−95% of DNA being encapsulated for all systems. Additional experiments with single-stranded mRNA also showed the formation of stable lipid nanoparticles formation in the 110−140 nm size range, which illustrates the potential for discrete lipid-PEG branched copolymers to be used for gene delivery.

As detailed previously, the presence of the bromo chain end allows for the facile introduction of labeling or targeting agents through azide substitution and subsequent click coupling (Figure 9).[54] To demonstrate this functional versatility, 7-mer, **DMG-(PEG4)$_7$-N$_3$** (28 EO), was prepared and incorporated into mixed lipid nanoparticles with the corresponding nonfunctional derivative, **DMG-(PEG4)$_7$-H**, (1:4 ratio) using the above procedures. Through strain-promoted azide−alkyne cycloaddition (SPAAC) chemistry, the lipid nanoparticles were functionalized by stepwise reaction of the azido chain end group with a dibenzocyclooctyne (DBCO) sulfo-cyanine3 derivative for fluorescence labeling and a dibenzocyclooctyne (DBCO) immunoglobulin G (IgG) derivative for targeting (see details in the Supporting Information).[55,56] After conjugation with both fluorescent and targeting groups, the lipid nanoparticles were shifted to 96-well plates coated with protein G, which selectively binds IgG. As shown in Figure 9, the lipid nanoparticle assembled from the **DMG-(PEG4)$_7$-N$_3$** derivative exhibited strong fluorescence when compared to the control system with no added **DMG-(PEG4)$_7$-N$_3$**. These results illustrate the successful conjugation of both the cyanine dye and the IgG antibody to the surface of lipid nanoparticles, with the IgG antibody remaining active for directed binding to 96-well plate surfaces functionalized with protein G. The modularity of this assay demonstrates the potential of these well-defined oligomers for developing multifunctional building blocks for a variety of applications.

CONCLUSIONS

A novel strategy for the scalable synthesis of multiple libraries of discrete lipid-PEG derivatives based on a DMG (lipid) functionalized ATRP initiator and tri- or tetra(ethylene glycol)acrylate repeat units is described. Key to the success of this approach is the combination of controlled polymerization with automated chromatographic separation. In-depth characterization confirms the discrete nature of the DMG-PEG derivatives with well-defined chain ends and accurate control over the total number of EO repeat units (12−36). The evaluation of these amphiphilic lipid-PEG libraries illustrates distinct trends, with the solution assembly behavior being influenced by the number of ethylene glycol units and the ω-chain end (−Br or −H). A comparison with commercial linear

https://doi.org/10.1021/jacs.2c07859
J. Am. Chem. Soc. XXXX, XXX, XXX−XXX

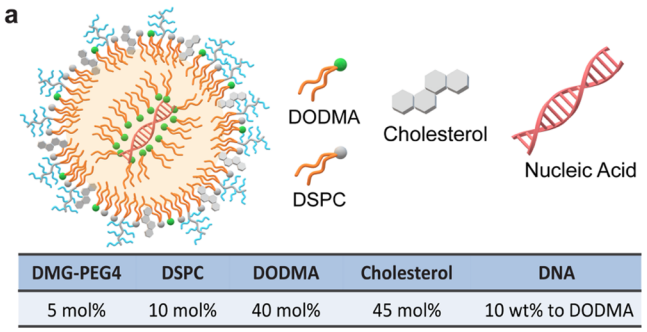

DMG-PEG4	DSPC	DODMA	Cholesterol	DNA
5 mol%	10 mol%	40 mol%	45 mol%	10 wt% to DODMA

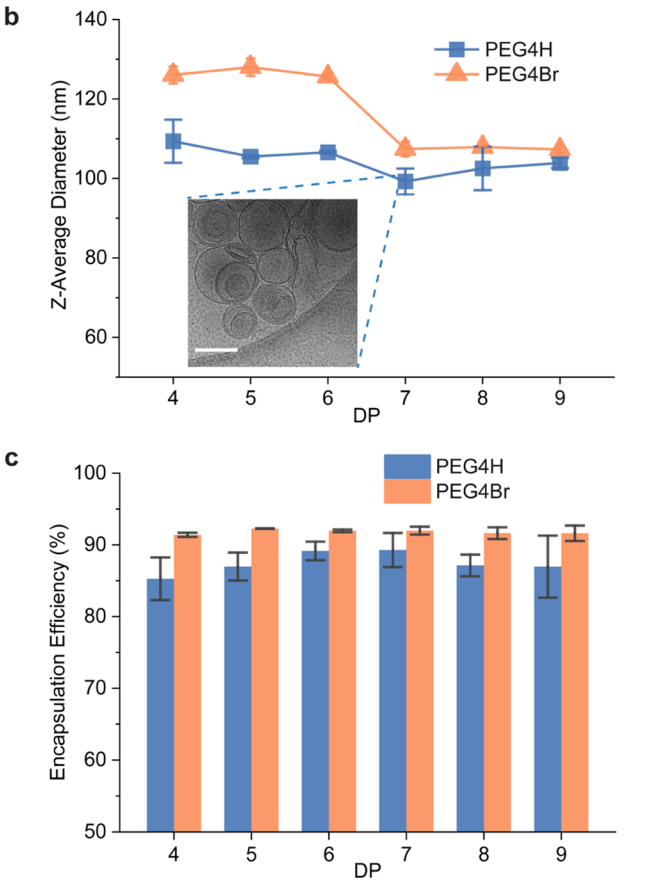

Figure 8. Lipid nanoparticles. (a) Formulation of LNPs. (b) Hydrodynamic diameters of the LNPs measured using DLS. The inset image was captured through cryo-TEM using sample **DMG-(PEG4)$_7$-H**; scale bar = 200 nm. (c) Nucleic acid encapsulation efficiency. The error bar represents the standard derivation of three measurements.

DMG-PEG2000 conjugates used in mRNA therapeutics shows a similar ability to form lipid nanoparticles with nucleic acids and tunable/low levels of protein absorption. However, reduced anti-PEG antibody binding is observed compared to the commercial linear PEG materials, consistent with their branched and discrete structure. This rapid discovery process facilitates the synthesis of ethylene glycol (EG) copolymer libraries with precise control over the structure and molecular weight. The availability of these discrete libraries enables fundamental structure/property relationships to be determined and comparisons with commercially important linear PEG derivatives, widely used in materials and pharmaceutical applications, realized.

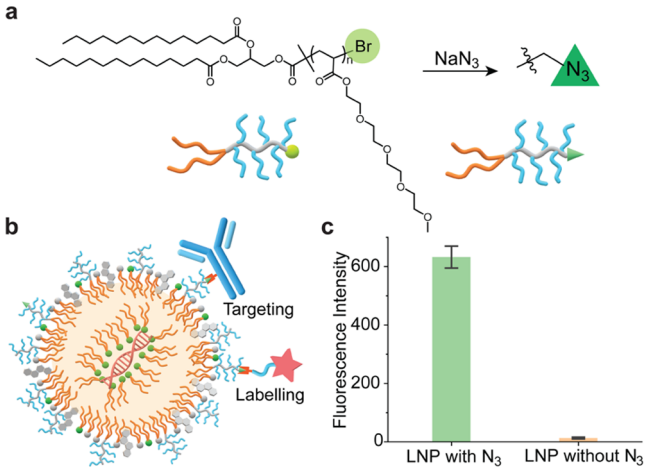

Figure 9. Diversification through click chemistry. (a) Preparation of the azido-ended oligomers. (b) Schematic illustration of LNP fluorophore labeling and antibody-directed targeting through click chemistry. (c) Fluorescence intensity of labeled LNPs incubated in the protein G-coated 96-well plates. The error bar represents the standard derivation of three measurements.

■ ASSOCIATED CONTENT

Supporting Information

The Supporting Information is available free of charge at https://pubs.acs.org/doi/10.1021/jacs.2c07859.

General experimental procedures and detailed synthetic procedures and characterization and additional data (PDF)

■ AUTHOR INFORMATION

Corresponding Author

Craig J. Hawker − *Materials Department, Materials Research Laboratory, and Department of Chemistry and Biochemistry, University of California, Santa Barbara, Santa Barbara, California 93106, United States;* orcid.org/0000-0001-9951-851X; Email: hawker@mrl.ucsb.edu

Authors

Junfeng Chen − *Materials Department, Materials Research Laboratory, and Department of Chemistry and Biochemistry, University of California, Santa Barbara, Santa Barbara, California 93106, United States*

Aoon Rizvi − *Department of Chemistry, University of California, Irvine, Irvine, California 92697, United States;* orcid.org/0000-0002-0022-1773

Joseph P. Patterson − *Department of Chemistry, University of California, Irvine, Irvine, California 92697, United States;* orcid.org/0000-0002-1975-1854

Complete contact information is available at: https://pubs.acs.org/10.1021/jacs.2c07859

Notes

The authors declare no competing financial interest.

■ ACKNOWLEDGMENTS

The research reported here was primarily supported by the National Science Foundation Materials Research Science and Engineering Center (MRSEC) at UC Santa Barbara (DMR-1720256, IRG-3) and the BioPACIFIC Materials Innovation Platform of the National Science Foundation under Award No.

DMR-1933487. The research reported here made use of shared facilities of the UC Santa Barbara MRSEC (NSF DMR-1720256), a member of the Materials Research Facilities Network (www.mrfn.org).

REFERENCES

(1) Siegwart, D. J.; Oh, J. K.; Matyjaszewski, K. ATRP in the design of functional materials for biomedical applications. *Prog. Polym. Sci.* **2012**, *37*, 18−37.
(2) Bielawski, C. W.; Grubbs, R. H. Living Ring-Opening Metathesis Polymerization. *Prog. Polym. Sci.* **2007**, *32*, 1−29.
(3) Lutz, J.-F.; Ouchi, M.; Liu, D. R.; Sawamoto, M. Sequence-Controlled Polymers. *Science* **2013**, *341*, No. 1238149.
(4) Moad, G.; Rizzardo, E.; Thang, S. H. Living Radical Polymerization by the RAFT Process. *Aust. J. Chem.* **2005**, *58*, 379−410.
(5) van Genabeek, B.; de Waal, B. F. M.; Gosens, M. M. J.; Pitet, L. M.; Palmans, A. R. A.; Meijer, E. W. Synthesis and Self-Assembly of Discrete Dimethylsiloxane−Lactic Acid Diblock Co-oligomers: The Dononacontamer and Its Shorter Homologues. *J. Am. Chem. Soc.* **2016**, *138*, 4210−4218.
(6) Barnes, J. C.; Ehrlich, D. J. C.; Gao, A. X.; Leibfarth, F. A.; Jiang, Y.; Zhou, E.; Jamison, T. F.; Johnson, J. A. Iterative exponential growth of stereo- and sequence-controlled polymers. *Nat. Chem.* **2015**, *7*, 810−815.
(7) Sun, Y.; Tan, R.; Ma, Z.; Gan, Z.; Li, G.; Zhou, D.; Shao, Y.; Zhang, W.-B.; Zhang, R.; Dong, X.-H. Discrete Block Copolymers with Diverse Architectures: Resolving Complex Spherical Phases with One Monomer Resolution. *ACS Cent. Sci.* **2020**, *6*, 1386−1393.
(8) Sellaturay, P.; Nasser, S.; Ewan, P. Polyethylene Glycol−Induced Systemic Allergic Reactions (Anaphylaxis). *J. Allergy Clin. Immunol. Pract.* **2021**, *9*, 670−675.
(9) Pozzi, D.; Colapicchioni, V.; Caracciolo, G.; Piovesana, S.; Capriotti, A. L.; Palchetti, S.; De Grossi, S.; Riccioli, A.; Amenitsch, H.; Laganà, A. Effect of polyethyleneglycol (PEG) chain length on the bio−nano-interactions between PEGylated lipid nanoparticles and biological fluids: from nanostructure to uptake in cancer cells. *Nanoscale* **2014**, *6*, 2782−2792.
(10) Sifri, R. J.; Padilla-Vélez, O.; Coates, G. W.; Fors, B. P. Controlling the Shape of Molecular Weight Distributions in Coordination Polymerization and Its Impact on Physical Properties. *J. Am. Chem. Soc.* **2020**, *142*, 1443−1448.
(11) Harris, J. M.; Chess, R. B. Effect of pegylation on pharmaceuticals. *Nat. Rev. Drug Discovery* **2003**, *2*, 214−221.
(12) Veronese, F. M.; Mero, A. The Impact of PEGylation on Biological Therapies. *BioDrugs* **2008**, *22*, 315−329.
(13) Detering, L.; Abdilla, A.; Luehmann, H. P.; Williams, J. W.; Huang, L.-H.; Sultan, D.; Elvington, A.; Heo, G. S.; Woodard, P. K.; Gropler, R. J.; Randolph, G. J.; Hawker, C. J.; Liu, Y. CC Chemokine Receptor 5 Targeted Nanoparticles Imaging the Progression and Regression of Atherosclerosis Using Positron Emission Tomography/Computed Tomography. *Mol. Pharmaceutics* **2021**, *18*, 1386−1396.
(14) Kulkarni, J. A.; Witzigmann, D.; Chen, S.; Cullis, P. R.; van der Meel, R. Lipid Nanoparticle Technology for Clinical Translation of siRNA Therapeutics. *Acc. Chem. Res.* **2019**, *52*, 2435−2444.
(15) Tenchov, R.; Bird, R.; Curtze, A. E.; Zhou, Q. Lipid Nanoparticles—From Liposomes to mRNA Vaccine Delivery, a Landscape of Research Diversity and Advancement. *ACS Nano* **2021**, *15*, 16982−17015.
(16) Hou, X.; Zaks, T.; Langer, R.; Dong, Y. Lipid nanoparticles for mRNA delivery. *Nat. Rev. Mater.* **2021**, *6*, 1078−1094.
(17) Chen, B.-M.; Cheng, T.-L.; Roffler, S. R. Polyethylene Glycol Immunogenicity: Theoretical, Clinical, and Practical Aspects of Anti-Polyethylene Glycol Antibodies. *ACS Nano* **2021**, *15*, 14022−14048.
(18) Cabanillas, B.; Novak, N. Allergy to COVID-19 vaccines: A current update. *Allergol. Int.* **2021**, *70*, 313−318.
(19) Sellaturay, P.; Nasser, S.; Islam, S.; Gurugama, P.; Ewan, P. W. Polyethylene glycol (PEG) is a cause of anaphylaxis to the Pfizer/BioNTech mRNA COVID-19 vaccine. *Clin. Exp. Allergy* **2021**, *51*, 861−863.
(20) Yang, Q.; Jacobs, T. M.; McCallen, J. D.; Moore, D. T.; Huckaby, J. T.; Edelstein, J. N.; Lai, S. K. Analysis of Pre-existing IgG and IgM Antibodies against Polyethylene Glycol (PEG) in the General Population. *Anal. Chem.* **2016**, *88*, 11804−11812.
(21) Sherman, M. R.; Williams, L. D.; Sobczyk, M. A.; Michaels, S. J.; Saifer, M. G. P. Role of the Methoxy Group in Immune Responses to mPEG-Protein Conjugates. *Bioconjugate Chem.* **2012**, *23*, 485−499.
(22) Saifer, M. G. P.; Williams, L. D.; Sobczyk, M. A.; Michaels, S. J.; Sherman, M. R. Selectivity of binding of PEGs and PEG-like oligomers to anti-PEG antibodies induced by methoxyPEG-proteins. *Mol. Immunol.* **2014**, *57*, 236−246.
(23) McSweeney, M. D.; Price, L. S. L.; Wessler, T.; Ciociola, E. C.; Herity, L. B.; Piscitelli, J. A.; DeWalle, A. C.; Harris, T. N.; Chan, A. K. P.; Saw, R. S.; Hu, P.; Jennette, J. C.; Forest, M. G.; Cao, Y.; Montgomery, S. A.; Zamboni, W. C.; Lai, S. K. Overcoming anti-PEG antibody mediated accelerated blood clearance of PEGylated liposomes by pre-infusion with high molecular weight free PEG. *J. Controlled Release* **2019**, *311*−*312*, 138−146.
(24) Ju, Y.; Lee, W. S.; Pilkington, E. H.; Kelly, H. G.; Li, S.; Selva, K. J.; Wragg, K. M.; Subbarao, K.; Nguyen, T. H. O.; Rowntree, L. C.; Allen, L. F.; Bond, K.; Williamson, D. A.; Truong, N. P.; Plebanski, M.; Kedzierska, K.; Mahanty, S.; Chung, A. W.; Caruso, F.; Wheatley, A. K.; Juno, J. A.; Kent, S. J. Anti-PEG Antibodies Boosted in Humans by SARS-CoV-2 Lipid Nanoparticle mRNA Vaccine. *ACS Nano* **2022**, *16*, 11769−11780.
(25) Bohn, P.; Meier, M. A. R. Uniform poly(ethylene glycol): a comparative study. *Polym. J.* **2020**, *52*, 165−178.
(26) Kinbara, K. Monodisperse engineered PEGs for bio-related applications. *Polym. J.* **2018**, *50*, 689−697.
(27) French, A. C.; Thompson, A. L.; Davis, B. G. High-Purity Discrete PEG-Oligomer Crystals Allow Structural Insight. *Angew. Chem., Int. Ed.* **2009**, *48*, 1248−1252.
(28) Geng, Z.; Lee, J.; Hawker, C. J. Placing Functionality Where You Want: The Allure of Sequence Control. *Chem* **2019**, *5*, 2510−2512.
(29) Binauld, S.; Damiron, D.; Connal, L. A.; Hawker, C. J.; Drockenmuller, E. Precise Synthesis of Molecularly Defined Oligomers and Polymers by Orthogonal Iterative Divergent/Convergent Approaches. *Macromol. Rapid Commun.* **2011**, *32*, 147−168.
(30) Gutekunst, W. R.; Hawker, C. J. A General Approach to Sequence-Controlled Polymers Using Macrocyclic Ring Opening Metathesis Polymerization. *J. Am. Chem. Soc.* **2015**, *137*, 8038−8041.
(31) Lawrence, J.; Lee, S.-H.; Abdilla, A.; Nothling, M. D.; Ren, J. M.; Knight, A. S.; Fleischmann, C.; Li, Y.; Abrams, A. S.; Schmidt, B. V. K. J.; Hawker, M. C.; Connal, L. A.; McGrath, A. J.; Clark, P. G.; Gutekunst, W. R.; Hawker, C. J. A Versatile and Scalable Strategy to Discrete Oligomers. *J. Am. Chem. Soc.* **2016**, *138*, 6306−6310.
(32) Lawrence, J.; Goto, E.; Ren, J. M.; McDearmon, B.; Kim, D. S.; Ochiai, Y.; Clark, P. G.; Laitar, D.; Higashihara, T.; Hawker, C. J. A Versatile and Efficient Strategy to Discrete Conjugated Oligomers. *J. Am. Chem. Soc.* **2017**, *139*, 13735−13739.
(33) Ren, J. M.; Lawrence, J.; Knight, A. S.; Abdilla, A.; Zerdan, R. B.; Levi, A. E.; Oschmann, B.; Gutekunst, W. R.; Lee, S.-H.; Li, Y.; McGrath, A. J.; Bates, C. M.; Qiao, G. G.; Hawker, C. J. Controlled Formation and Binding Selectivity of Discrete Oligo(methyl methacrylate) Stereocomplexes. *J. Am. Chem. Soc.* **2018**, *140*, 1945−1951.
(34) Huang, Z.; Noble, B. B.; Corrigan, N.; Chu, Y.; Satoh, K.; Thomas, D. S.; Hawker, C. J.; Moad, G.; Kamigaito, M.; Coote, M. L.; Boyer, C.; Xu, J. Discrete and Stereospecific Oligomers Prepared by Sequential and Alternating Single Unit Monomer Insertion. *J. Am. Chem. Soc.* **2018**, *140*, 13392−13406.
(35) Zhang, C.; Bates, M. W.; Geng, Z.; Levi, A. E.; Vigil, D.; Barbon, S. M.; Loman, T.; Delaney, K. T.; Fredrickson, G. H.; Bates, C. M.; Whittaker, A. K.; Hawker, C. J. Rapid Generation of Block

https://doi.org/10.1021/jacs.2c07859
J. Am. Chem. Soc. XXXX, XXX, XXX−XXX

Copolymer Libraries Using Automated Chromatographic Separation. *J. Am. Chem. Soc.* **2020**, *142*, 9843−9849.
(36) Zhang, C.; Vigil, D. L.; Sun, D.; Bates, M. W.; Loman, T.; Murphy, E. A.; Barbon, S. M.; Song, J.-A.; Yu, B.; Fredrickson, G. H.; Whittaker, A. K.; Hawker, C. J.; Bates, C. M. Emergence of Hexagonally Close-Packed Spheres in Linear Block Copolymer Melts. *J. Am. Chem. Soc.* **2021**, *143*, 14106−14114.
(37) Rissler, K.; Wyttenbach, N.; Börnsen, K. O. High-performance liquid chromatography of polyethylene glycols as their α,ω-bis(1-naphthylurethane) derivatives and signal monitoring by fluorescence detection. *J. Chromatogr. A* **1998**, *822*, 189−206.
(38) Gill, K. K.; Kaddoumi, A.; Nazzal, S. PEG−lipid micelles as drug carriers: physiochemical attributes, formulation principles and biological implication. *J. Drug Target.* **2015**, *23*, 222−231.
(39) Fang, Q.; Chen, T.; Zhong, Q.; Wang, J. Thermoresponsive polymers based on oligo(ethylene glycol) methyl ether methacrylate and modified substrates with thermosensitivity. *Macromol. Res.* **2017**, *25*, 206−213.
(40) Becer, C. R.; Hahn, S.; Fijten, M. W. M.; Thijs, H. M. L.; Hoogenboom, R.; Schubert, U. S. Libraries of methacrylic acid and oligo(ethylene glycol) methacrylate copolymers with LCST behavior. *J. Polym. Sci., Part A: Polym. Chem.* **2008**, *46*, 7138−7147.
(41) Luchini, A.; Vitiello, G. Understanding the Nano-bio Interfaces: Lipid-Coatings for Inorganic Nanoparticles as Promising Strategy for Biomedical Applications. *Front. Chem.* **2019**, *7*, 343.
(42) Thakur, N. S.; Patel, G.; Kushwah, V.; Jain, S.; Banerjee, U. C. Self-Assembled Gold Nanoparticle−Lipid Nanocomposites for On-Demand Delivery, Tumor Accumulation, and Combined Photothermal−Photodynamic Therapy. *ACS Appl. Bio Mater.* **2019**, *2*, 349−361.
(43) Mieszawska, A. J.; Gianella, A.; Cormode, D. P.; Zhao, Y.; Meijerink, A.; Langer, R.; Farokhzad, O. C.; Fayad, Z. A.; Mulder, W. J. M. Engineering of lipid-coated PLGA nanoparticles with a tunable payload of diagnostically active nanocrystals for medical imaging. *Chem. Commun.* **2012**, *48*, 5835−5837.
(44) Lu, Y.; Yue, Z.; Xie, J.; Wang, W.; Zhu, H.; Zhang, E.; Cao, Z. Micelles with ultralow critical micelle concentration as carriers for drug delivery. *Nat. Biomed. Eng.* **2018**, *2*, 318−325.
(45) Heywood, B. R.; Mann, S. Template-directed nucleation and growth of inorganic materials. *Adv. Mater.* **1994**, *6*, 9−20.
(46) Jana, N. R.; Gearheart, L.; Murphy, C. J. Seed-Mediated Growth Approach for Shape-Controlled Synthesis of Spheroidal and Rod-like Gold Nanoparticles Using a Surfactant Template. *Adv. Mater.* **2001**, *13*, 1389−1393.
(47) Hou, Y.; Zhou, Y.; Wang, H.; Sun, J.; Wang, R.; Sheng, K.; Yuan, J.; Hu, Y.; Chao, Y.; Liu, Z.; Lu, H. Therapeutic Protein PEPylation: The Helix of Nonfouling Synthetic Polypeptides Minimizes Antidrug Antibody Generation. *ACS Cent. Sci.* **2019**, *5*, 229−236.
(48) Cooper, M. A.; Try, A. C.; Carroll, J.; Ellar, D. J.; Williams, D. H. Surface plasmon resonance analysis at a supported lipid monolayer. *Biochim. Biophys. Acta* **1998**, *1373*, 101−111.
(49) Zhang, P.; Sun, F.; Hung, H.-C.; Jain, P.; Leger, K. J.; Jiang, S. Sensitive and Quantitative Detection of Anti-Poly(ethylene glycol) (PEG) Antibodies by Methoxy-PEG-Coated Surface Plasmon Resonance Sensors. *Anal. Chem.* **2017**, *89*, 8217−8222.
(50) Qi, Y.; Simakova, A.; Ganson, N. J.; Li, X.; Luginbuhl, K. M.; Ozer, I.; Liu, W.; Hershfield, M. S.; Matyjaszewski, K.; Chilkoti, A. A brush-polymer/exendin-4 conjugate reduces blood glucose levels for up to five days and eliminates poly(ethylene glycol) antigenicity. *Nat. Biomed. Eng.* **2017**, *1*, 0002.
(51) Richter, A. W.; Åkerblom, E. Antibodies against Polyethylene Glycol Produced in Animals by Immunization with Monomethoxy Polyethylene Glycol Modified Proteins. *Int. Arch. Allergy Immunol.* **1983**, *70*, 124−131.
(52) Li, H.; Piao, L.; Yu, B.; Yung, B. C.; Zhang, W.; Wang, P. G.; Lee, J. L.; Lee, R. J. Delivery of calf thymus DNA to tumor by folate receptor targeted cationic liposomes. *Biomaterials* **2011**, *32*, 6614−6620.
(53) Oberli, M. A.; Reichmuth, A. M.; Dorkin, J. R.; Mitchell, M. J.; Fenton, O. S.; Jaklenec, A.; Anderson, D. G.; Langer, R.; Blankschtein, D. Lipid Nanoparticle Assisted mRNA Delivery for Potent Cancer Immunotherapy. *Nano Lett.* **2017**, *17*, 1326−1335.
(54) Kolb, H. C.; Finn, M. G.; Sharpless, K. B. Click Chemistry: Diverse Chemical Function from a Few Good Reactions. *Angew. Chem., Int. Ed.* **2001**, *40*, 2004−2021.
(55) Agard, N. J.; Prescher, J. A.; Bertozzi, C. R. A Strain-Promoted [3 + 2] Azide−Alkyne Cycloaddition for Covalent Modification of Biomolecules in Living Systems. *J. Am. Chem. Soc.* **2004**, *126*, 15046−15047.
(56) Baskin, J. M.; Prescher, J. A.; Laughlin, S. T.; Agard, N. J.; Chang, P. V.; Miller, I. A.; Lo, A.; Codelli, J. A.; Bertozzi, C. R. Copper-free click chemistry for dynamic in vivo imaging. *Proc. Natl. Acad. Sci. U.S.A.* **2007**, *104*, 16793−16797.

Recommended by ACS

Discrete, Chiral Polymer–Insulin Conjugates
Wencong Wang, Jeremiah A. Johnson, *et al.*
SEPTEMBER 20, 2022
JOURNAL OF THE AMERICAN CHEMICAL SOCIETY
READ

Star Polymer Nanomedicines—Challenges and Future Perspectives
Helen Forgham, Thomas P. Davis, *et al.*
SEPTEMBER 01, 2022
ACS APPLIED POLYMER MATERIALS
READ

Mechanistic Influence of Polymer Species, Molecular Weight, and Functionalization on Mucin–Polymer Binding Interactions
Jeffrey Watchorn, Frank X. Gu, *et al.*
SEPTEMBER 15, 2022
ACS APPLIED POLYMER MATERIALS
READ

Probing Crowdedness of Artificial Organelles by Clustering Polymersomes for Spatially Controlled and pH-Triggered Enzymatic Reactions
Peng Wang, Dietmar Appelhans, *et al.*
AUGUST 18, 2022
BIOMACROMOLECULES
READ

Get More Suggestions >

https://doi.org/10.1021/jacs.2c07859
J. Am. Chem. Soc. XXXX, XXX, XXX−XXX